

Minimization of sound radiation in doubly curved shallow shells by means of structural stiffness

Tomás MENDEZ ECHENAGUCIA^{1*}, N.B. ROOZEN², Philippe BLOCK¹

^{1*} ETH Zurich, Institute of Technology in Architecture, Block Research Group
Stefano-Franscini-Platz 1, HIB E 46, 8093 Zurich, Switzerland
mendez@arch.ethz.ch

² KU Leuven, Department of Physics and Astronomy, Leuven, Belgium

Abstract

A large amount of the embedded energy of buildings is due to their structures. Consequently, designers have been developing lighter and material efficient structures. However, lightweight structures are vulnerable to aerial and structure-borne noise transmission, especially for the lower frequencies. Sound insulation from environmental noise or footfall is commonly addressed by increasing the mass of the structure, resulting in inefficient constructions. In the lower frequency range, structural stiffness plays a significant role in preventing sound transmission. This paper studies the relationship between stiffness and the acoustical insulation properties of shallow structural shells. The sound radiation of doubly curved shells, under point loads, is estimated by computing the surface normal velocity using Finite Element Method and the radiated sound power using the Rayleigh Integral. The paper shows the potential of optimizing shallow shells for sound transmission by means of their shape, the distribution of mass, and the topology of stiffening ribs.

1. Introduction

As the operational energy in buildings is significantly reduced by more efficient thermal insulation, heating and cooling systems as well as on site energy generation, the embedded energy becomes a larger percentage of the carbon footprint of buildings. The embedded energy of buildings is vastly determined by their structure (Kaethner and Burrige [1]), and in particular, floor slabs contribute a large amount of this energy (De Wolf et al. [2]). For this reason, significant efforts have been made in the reduction of material quantities by means of structural optimization, resulting in increasingly lighter structures.

An example of a lightweight structural system is the funicular floor system developed by the Block Research Group for the NEST HiLo research unit in Dübendorf, Switzerland (López López et al. [3]). This slab consists of a shallow funicular shell, generated by means of Thrust Network Analysis (TNA) (Block [4]), a series of stiffening ribs, and tension ties. The shell and ribs are both made in 2cm thick unreinforced concrete. This results in a floor system that has 70% less concrete than a traditional 25-30 cm thick slab for standard spans. This significant reduction in mass poses the problem of the sound insulation of the floor system, especially in the low frequency range. In addition to damping, the sound insulation of building partitions such as walls and slabs relies heavily on their mass. Floor slabs, for example, have traditionally been built with thick concrete slabs, and sometimes additional screed layers are added to increase the mass and reduce sound transmission, significantly increasing their weight and carbon footprint.

Doubly curved surfaces are much stiffer when compared to flat surfaces of the same material and thickness. Research in the aerospace industry has yielded powerful numerical methods for computing sound transmission for complex shapes as well as great results in minimizing the acoustic radiation of panels in the low frequency range by means of stiffness (Ng and Hui [5], Joshi et al [6,7]). However stiffness is neglected in the building sector as most partitions are flat. Similarly, shell structures are usually designed and optimized for structural efficiency and rarely for acoustic insulation.

This paper proposes the minimization of the sound radiation of shallow shells by means of optimizing their shape, mass distribution and rib-stiffeners patterns. The acoustic radiation of shallow shells under point excitations is computed by means of the Rayleigh Integral (Koopmann and Benner [8], Fahy and Gardonio [9]), in combination with the Finite Element Method.

The paper presents three numerical experiments that study the potential of structural stiffness for sound insulation. The first experiment compares shallow shell shapes of different heights with a flat surface of the same thickness, as well as to flat surfaces of much higher thicknesses. The shallow shell shapes are generated by means of TNA, so that they represent compression-only solutions for their self-weight. The second experiment studies the potential of distributing the mass of a flat surface in a pattern that minimizes the acoustic radiation. The optimal mass distribution is found by means of Genetic Algorithms (Goldberg [10]). The third and final experiment studies the potential of stiffening ribs, in their shape and topology, by comparing two different rib-stiffened shells of equal mass. One of the shells is based on the NEST HiLo funicular floor system, while the other one is a simple grid pattern.

2. Methodology

To investigate the potential of structural stiffness for the sound insulation of lightweight shell structures in the low frequency range, this paper evaluates three different approaches: shape, mass distribution and rib-stiffener pattern. All three approaches require an adequate vibro-acoustic model to estimate sound radiation from these shells, which is done by means of the Rayleigh Integral. This method has the advantage of being computationally inexpensive while still being precise enough for the purposes of optimization. This method does not account for room acoustic effects, the radiated sound power is a single quantity number that is representative for the sound pressure in the so-called far-field. However, for optimization purposes this is considered to be a reasonable quantity to minimize the overall level in the room.

The first and last approach require a form-finding technique to generate shell shapes, which is done by means of TNA. The mass distribution approach requires a robust optimization strategy, for which genetic algorithms are employed.

2.1. Vibro Acoustic simulation

Considering two rooms (source and receiver) that are connected by a sound transmitting partition, the three main elements are required to estimate the sound power radiated by the partition: (i) the simulation of the sound sources in the source room (or acoustic load), (ii) the mechanical behaviour of the partition (the structural response), and (iii) the radiation that results from the vibration of the partition (the acoustical response). This section outlines how each one of these elements are implemented in this paper.

2.1.1. The acoustic response: The Rayleigh Integral model

The sound power radiated from shallow shell structures can be estimated with the approach outlined in (Bai and Tsao 2002 [11]), which is based on the so-called Rayleigh Integral (Koopmann and Benner [8], Fahy and Gardonio [9]). In this approach, a baffled surface that is subjected to acoustic excitation on one side and is radiating sound energy into the other side, is considered. The other side is considered a half-space that is filled with air. If we consider the radiating surface to be subdivided into planar

segments or elements, the sound power (W), radiated by the surface into the air filled half-space in a particular frequency (f), can be estimated by:

$$W = \frac{S}{2} \text{Re}\{\mathbf{v}^H \mathbf{p}\} \quad (1)$$

where S is the area of each element, \mathbf{p} and \mathbf{v} are the pressure and surface velocity vectors at each element, and the superscript ‘‘H’’ corresponds to the Hermitian transpose of the vector. The calculation of W is done per frequency and in this paper the lower end of the sound spectrum is the most relevant one. The pressure vector can then be obtained as such (Bai and Tsao 2002 [11], Berkhoff [12]):

$$\mathbf{p} = \mathbf{Z}\mathbf{v} \quad (2)$$

\mathbf{Z} is the so-called radiation impedance matrix and can be calculated for plates and shallow shells in the following way (Bai and Tsao 2002 [11]):

$$\mathbf{Z} = \rho_0 c \begin{bmatrix} d & -\frac{jkS}{2\pi} \frac{e^{ikr_{12}}}{r_{12}} & \dots & -\frac{jkS}{2\pi} \frac{e^{ikr_{1N}}}{r_{1N}} \\ -\frac{jkS}{2\pi} \frac{e^{ikr_{21}}}{r_{21}} & d & \dots & \vdots \\ \vdots & \vdots & \dots & \vdots \\ -\frac{jkS}{2\pi} \frac{e^{ikr_{2N}}}{r_{2N}} & \dots & \dots & d \end{bmatrix} \quad (3)$$

where:

$$d = \frac{1}{2} \left(k \sqrt{\frac{S}{\pi}} \right)^2 - j \frac{8}{3\pi} \left(k \sqrt{\frac{S}{\pi}} \right) \quad (4)$$

and $r_{[m,n]}$ is the geometric distance between the centre of mass of the m^{th} and n^{th} elements. There are two main unknowns in the model, \mathbf{Z} and \mathbf{v} . The radiation impedance matrix \mathbf{Z} can be calculated using only geometrical information, while \mathbf{v} requires the structural response. This means that if the geometry of the shells is the same, \mathbf{Z} needs to be calculated only once. This presents the opportunity to significantly reduce the computation time during mass distribution optimization.

2.1.2. The structural response: Finite Element Method

The mechanical behaviour of the doubly curved partitions considered in this paper is estimated by use of the Finite Element Method (FEM). In particular, the FEM simulation package ANSYS (Kohnke [13]) was employed. A harmonic analysis is performed to determine the steady-state response of the structure under harmonic loads. The velocity vector \mathbf{v} used in Equations 1 and 2, can be obtained directly from the FEM analysis using the linear displacements of the shell structure:

$$\mathbf{v} = \omega \mathbf{x} j = 2\pi f \mathbf{x} j \quad (5)$$

where ω is the angular velocity, \mathbf{x} is the complex displacement of each element in the surface, and j is $\sqrt{-1}$.

All of the numerical experiment in this paper use the same material properties for all of the studied shell structures. The material used is a concrete with an E modulus of 44 GPa, a Poisson ratio of 0.2 and a density of 2400 Kg/m³.

2.1.3. Sound sources

This paper studies the sound radiation of shallow shells under harmonic point loads. The FEM harmonic analysis assumes, by definition, that all loads applied vary sinusoidally with time. For this paper, a unit magnitude of varying frequency is used following Snyder and Tanaka [14] as well as Joshi et al. [7]. The frequencies studied in this paper range from 10 to 200 Hz, thus these are the frequencies used in the harmonic point loads.

2.2. Thrust Network Analysis

Thrust Network Analysis (TNA) is a form-finding method used for the generation of funicular discrete networks under vertical loading conditions (Block [4]). If Γ and Γ^* are two planar graphs with the same number of elements, and if Γ^* is the convex, parallel dual of Γ , then Γ and Γ^* are the form and force diagram of a three-dimensional thrust compression-only network G (Figure 1). This network is in equilibrium under vertical loads applied to its nodes, and has Γ as its horizontal projection and Γ^* as its horizontal equilibrium (Van Mele et al. [15]).

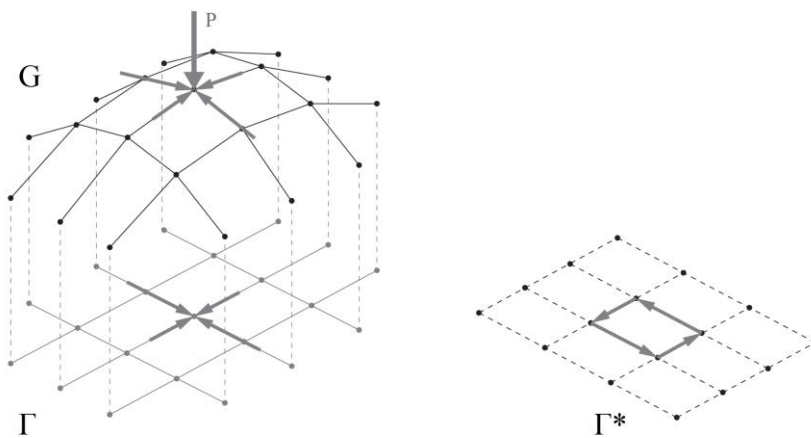


Figure 1: TNA dual graph, Thrust Network G , Form diagram Γ and Force diagram Γ^* .

The static indeterminacy of nodes in the thrust network with a valency higher than three allows for the existence of more than one force diagram Γ^* that satisfies the convexity and parallelity requirements for the network G to be in equilibrium in compression only. A longer force branch in Γ^* results in a shallower thrust network (Figure 2). This feature is exploited in TNA to generate different funicular shapes with the same form diagram, allowing the designer to explore multiple solutions. This feature is exploited in this paper to generate shell shapes of different heights with the exact same horizontal projection.

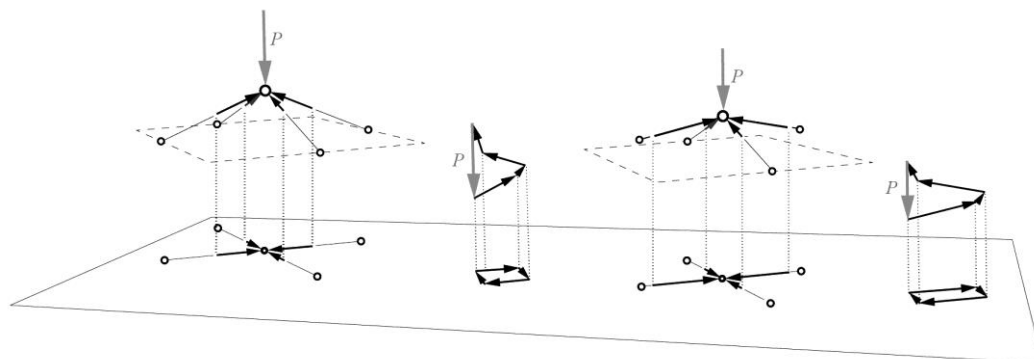


Figure 2: Indeterminacy of a four bar node (Block [4])

2.3. Genetic Algorithms

Genetic Algorithms (GAs) are a family of search algorithms based on natural selection the evolution of the species (Goldberg [10]). First proposed by John Holland in the mid 1970's in the University of Michigan, they have been successfully employed in many varied fields of study, including the architecture and construction field.

GAs generate new solutions a by the use of bits and pieces taken from the best of the previously considered solutions. These bits and pieces are taken from the problem variables. Like in all search algorithms, in GAs solutions to the given problem are characterized by a set of variables, and these variables are typically represented by numbers. These numbers are then coded. Following the biological analogies used to describe genetic algorithms, this code then becomes the genome of the individuals in the population. Like in nature, the offspring or new generation of individuals are made up from the genes of their parents. The success of the GA is related to the selection of the right parents, and the correct combination of their genes.

3. Minimization of sound radiation by structural stiffness

3.1. Experiment 1: Shell shapes

This numerical experiment presents the comparison of funicular shell shapes of different heights in terms of their sound radiation. The Rayleigh Integral approach described above, as well as TNA are used to generate shapes and analyse their acoustic response.

3.1.1. Comparison parameters and variables

Figure 3 shows the five shells considered for the shape analysis, they are all 5x5 m squares in plan. The first shell "a" is completely flat, while shells "b", "c", "d" and "e" are doubly curved with increasing height at the centre, from 0.1 to 0.4 m. All of the shapes are form found using TNA with the same form diagram (shown in Figure 3). All shells have a thickness of 2 cm, and are analysed, as detailed above, by means of the Rayleigh Integral and FE analysis to calculate their per frequency sound radiation W . All shapes are simply supported along the entire boundary, and are subjected to an asymmetric harmonic load, as indicated in Figure 3, as employed by Snyder and Tanaka [14], and Joshi et al. [7].

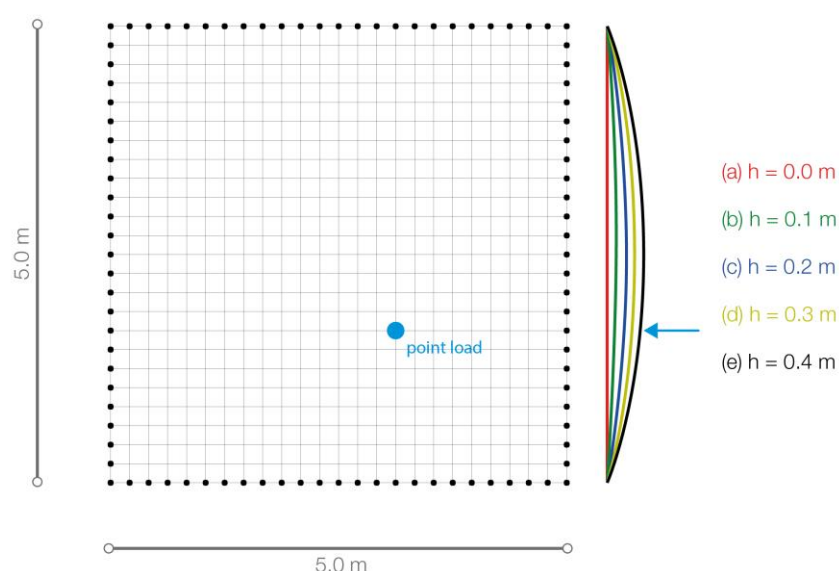


Figure 3: Shell shapes for sound radiation comparison

3.1.2. Results

While there is no optimization procedure being employed in this comparison, this parametric study is made to examine the potential of shape optimization to provide stiffness. Figures 4(a) and 4(b) show the results of this experiment. Figure 4(a) shows the total sound radiation W (dB) for all five shell structures from 10 to 200 Hz. It shows how the flat shell radiates over 10 dB more sound power in most sound frequencies when compared to the 0.3 m high shell, and over 20 dB more when compared to the 0.4 m high shell. This represents a significant reduction of sound energy without adding mass.

Figure 4(b) shows a comparison between the 0.4 m high doubly curved shell (shown in black), and flat shells of increasing mass. It can be seen that it takes an increase in mass of at least 4 times to achieve results as good as the curved shell. In other words, the shallow doubly curved shell can potentially save 4 times the mass with equal or superior acoustical insulation.

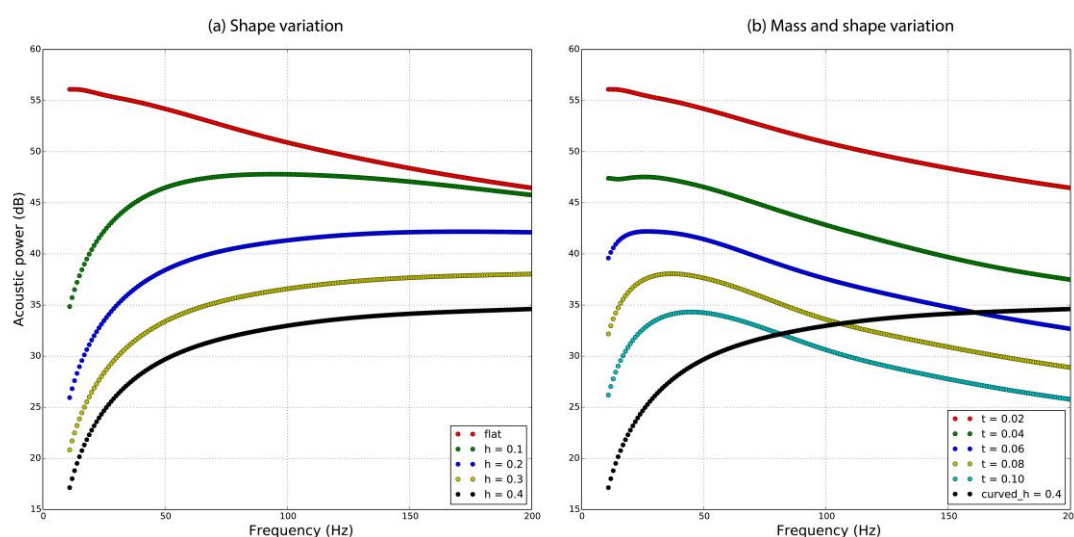


Figure 4: Results of Experiment 1: (a) shell shape variation, radiated acoustic power per frequency, (b) shell mass variation - comparison with 0.4m high shell, radiated acoustic power per frequency.

3.2. Experiment 2: Mass distribution

This experiment presents the minimization of sound radiation by distributing the mass in the different segments of a flat shell structure. Given a fixed amount of material, the objective is to find the optimal distribution of the material such that the radiation is as low as possible. The variables in this optimization problem are the thicknesses of each one of the planar faces of a given and fixed shell geometry, while still maintaining equal total mass.

3.2.1. Optimization parameters and variables

The optimization is done by means of GA. The GA was used in coordination with the Rayleigh integral and FEM acoustic simulation to generate radiation values for each proposed solution (or individual). Since the geometry of the shell is fixed, the radiation impedance matrix \mathbf{Z} is only calculated once at the beginning of the optimization. From that point on the only element required for the calculation of W is the velocities vector \mathbf{v} . This was calculated using the FEM analysis described above. Also in this experiment the shells were simply supported along the entire perimeter. The total mass for each shell is exactly the same, it is the mass that the shell would have if it were uniformly distributed with a thickness of 5 cm.

The surface used in this problem is the same flat surface used in the previous experiment (Figure 3). This surface has 576 faces, meaning that the GA has the task of finding the combination shell thicknesses for those 576 faces that minimizes sound radiation. In order to reduce the number of variables, the mass distribution patterns are assumed to be symmetrical in both X and Y axis, thus reducing the number of variables to $576/4 = 144$.

The fitness value used in the GA optimization is obviously related to the radiated sound power W , however, since this value is frequency dependent, there are many W values per solution. In this case the maximum W is assumed to be the fitness value. This means the optimal solution found may not have the lowest W for all frequencies, but the lowest maximum W . This also means that the lowest maximum W may not be found in the same frequency for all solutions. This simplification however does seem to produce optimal overall results.

The GA was setup to have a population made up of 50 individuals, with an elite population size of 10, and to run for 200 generations. A mutation operator was also employed to keep population diversity, by mutating 0.05% of all genes.

3.2.2. Results

Figure 5(a) shows the evolution on the mass distribution and the resulting patterns, the maximum W value is minimized progressively as the pattern is optimized. The GA evolution shows an improvement of maximum W of close to 6 dB. The mass distribution patterns show in black the highest thickness for each solution, in white the lowest thickness, and in grey the thicknesses in between. It can be seen that in the early generations of the evolutionary process, there are many grey areas, meaning that the mass distribution is closer to being uniform. In the more evolved solutions there is a higher contrast, the GA has found the most effective areas to invest the mass, and thus the patterns have larger black and white areas.

Figure 5(b) shows the radiated acoustic power of the optimized mass distribution, compared to the power radiated by the uniform thickness shell of the same mass. In it, we can see that the optimization process produces a shell that decreases the radiated acoustic power by up to 5 dB in most of the lower frequencies. This improvement is not as large as the one shown in the shape comparison, however, the potential of optimal mass distribution to increase stiffness is shown.

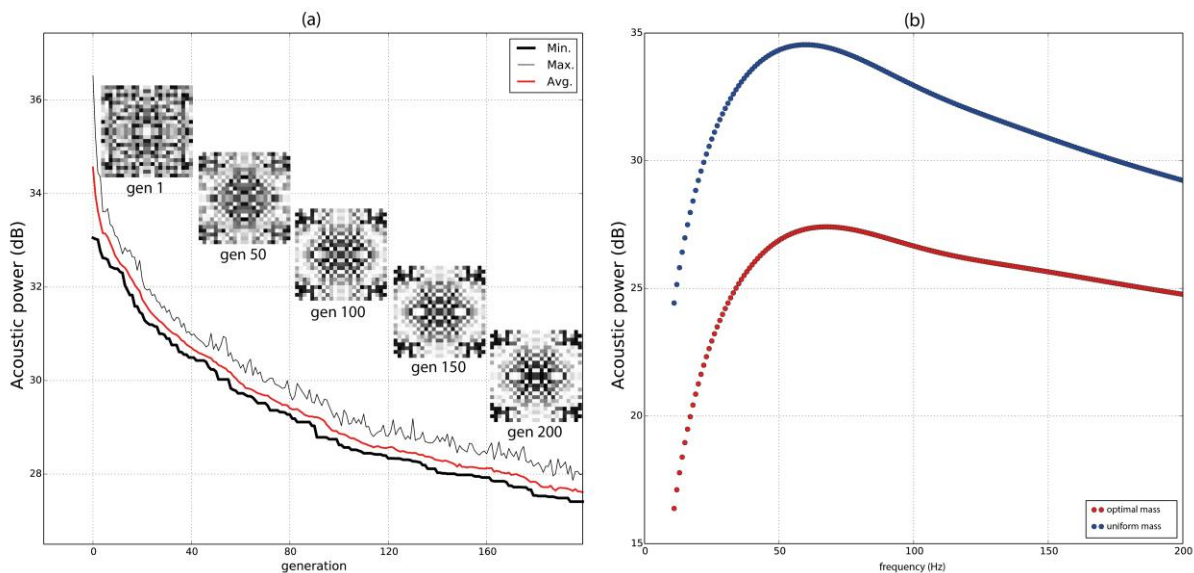


Figure 5: Results of Experiment 2: (a) GA minimum, maximum and average fitness values per generation, optimal mass distribution patterns for generations 1, 50, 150, 200. (b) Optimal mass distribution and uniform distribution comparison, radiated acoustic power per frequency.

3.3. Experiment 3: Pattern optimization, designing stiffening ribs.

The third experiment presented in this paper studies the potential of rib stiffeners to increase the sound insulating capabilities of shallow shells, specifically it compares two different patterns for these stiffeners.

3.3.1. Comparison parameters and variables

Figure 6 shows the two shells compared in this experiment. Shell (a) is a 5x5 m, doubly curved shell with a height of 0.3 m at the centre, with stiffening ribs arranged in a grid pattern, spaced 62.5 cm apart. Shell (b) is also a 5x5 m doubly curved shell with a height of 0.3 m at the centre, but the pattern of the stiffening ribs is different, it is the pattern used for the NEST HiLo funicular floor system described above. Both shells have a thickness of shell and ribs of 2 cm, and both have exactly the same mass. The Rayleigh Integral approach in combination with the FEM was also employed. Both shells were simply supported along the perimeter.

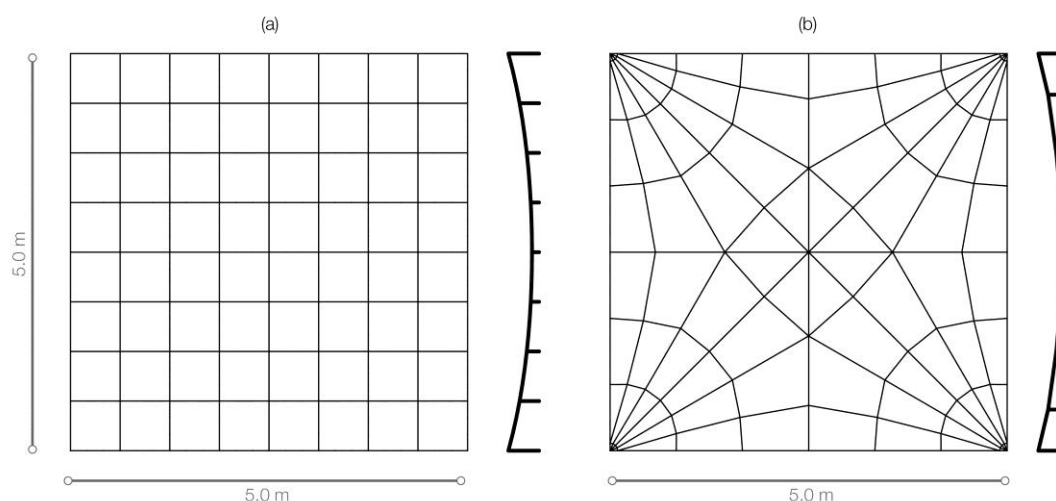


Figure 6: Rib-stiffeners pattern and sections: (a) grid stiffeners, $h = 0.3$ m, (b) NEST HiLo stiffeners, $h = 0.3$ m.

3.3.2. Results

Figure 7 shows the comparison of the radiated acoustic power for both shells per frequency. The first important result to notice is that compared to the 0.3 m high shell (without rib stiffeners) shown in Experiment 1, both patterns have a much lower acoustic radiation, thus showing the impact of the stiffeners. The results also show that the grid pattern radiates up to 5 dB more than the Hilo pattern in the low frequencies, highlighting the potential of optimizing the shape and topology of the ribs. This result agrees with the findings of Joshi et al. [7].

4. Conclusion

The numerical experiments shown in this paper demonstrate the high potential of using structural stiffness for the sound insulation of shallow shell structures for the lower frequencies. Three experiments are carried out to show this potential in terms of shape, mass distribution and the topology of stiffeners.

The optimization of shell shapes shows the most potential, obtaining reductions of up to 20 dB in most sound frequencies between a flat shell and a doubly curved shallow shell of equal thickness. The optimization of mass distribution shows that higher stiffness can also be achieved by using optimal distribution of mass in shell structures. These shells with non-uniform thicknesses are shown to have lower sound radiation values, by up to 5 dB. The comparison of different rib stiffeners pattern again shows that a stiffer

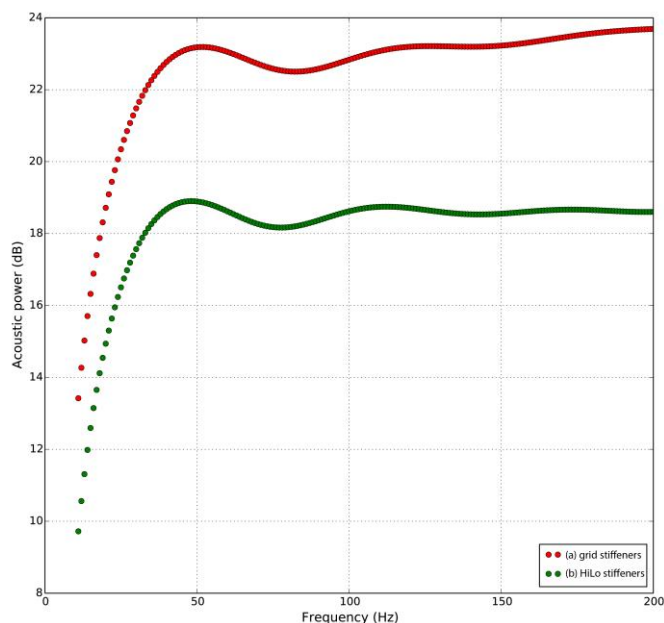


Figure 7: Result of Experiment 3: (a) grid stiffeners, acoustic power per frequency, (b) NEST HiLo stiffeners, acoustic power per frequency.

pattern achieves a better sound radiation result, in this case, an improvement of almost 5 dB in most of the lower frequencies.

The optimization of shell shapes seems to show the most potential, as the comparison with flat shapes shows by far the highest gain in insulation. However, mass distribution and stiffener configurations are also shown to have potential as optimization strategies, although less effective.

Future work includes the investigation of the effect of different boundary conditions, such as different supporting conditions and different acoustic cases, such as airborne noise loading cases. The scalability of the stiffness strategy should also be tested with larger spans, masses and shapes. Most importantly, an optimization strategy needs to be developed capable of optimizing shape to minimize sound radiation whilst maintaining structural capacity without increasing mass.

Future work also involves the determination of the radiated sound power of optimized structures in the higher frequency region. Whilst in the lower frequency range the stiffening effect of curvature, ribs and mass distribution reduces the radiated sound power, in the higher frequency range this might be different, amongst others due to a lowering of the critical frequency. Research into this to make a good trade-off between low- and high frequency performance of architectural structures is highly desired.

Acknowledgements

This research was funded by the Sustainable Construction Seed funding grant given by the ETH Zürich Foundation.

References

- [1] Kaethner SC, Burrige JA. Embodied CO₂ of structural frames, *The structural engineer*. 2012; **90**(5); 33-40.
- [2] De Wolf, C., Ramage, M. and Ochsendorf, J., Low Carbon Vaulted Masonry Structures, in *Proceedings of the IASS Annual Symposium 2016*, K. Kawaguchi, M. Ohsaki, T. Takeuchi (eds.), 2016.
- [3] López López D., Veenendaal D., Akbarzadeh M., and Block P. Prototype of an ultra-thin, concrete vaulted floor system, In *Proceedings of the IASS-SLTE 2014 Symposium*. Brasilia, Brazil, 2014.
- [4] Block, P., Thrust Network Analysis: Exploring Three-dimensional Equilibrium, PhD thesis, Massachusetts Institute of Technology, Cambridge, MA, 2009.
- [5] Ng, C.F. and Hui, C.K. Low-frequency sound insulation using stiffness control with honeycomb panels. *Applied Acoustics*, 2008; **69**(4); 293 - 301.
- [6] Joshi P., Mulani, S.B., Kapania, R.K. Multi-objective vibro-acoustic optimization of stiffened panels. *Structural and Multidisciplinary Optimization* 2015; **51**:835-848.
- [7] Joshi P., Mulani S., Gurav S.P., Kapania R.K., Design optimization for minimum sound radiation from point-excited curvilinearly stiffened panel. *Journal of Aircraft*. 2010; **47**: 1100-1110.
- [8] Koopmann, G.H. and Benner, H. Method for computing the sound power of machines based on the Helmholtz integral, *Journal of the Acoustical Society of America*. 1982; **71**(1).
- [9] Fahy F., Gardonio, P. Sound and structural vibration: radiation, transmission and response (2nd ed.). Academic Press, 2007
- [10] Goldberg, D., Genetic algorithms in Search, Optimization & Machine Learning, (1st ed), Addison-Wesley Professional, 1989.
- [11] Bai M.R., Tsao M., Estimation of sound power of baffled planar sources using radiation matrices. *Journal of the Acoustical Society of America*. 2002; **112**: 876-883.
- [12] Berkhoff A.P., Sensor scheme design for active structural acoustic control. *Journal of the Acoustical Society of America*. 2000; **108**: 1037-1045.
- [13] P. Kohnke, Theory Reference, ANSYS, 1994.
- [14] Snyder S., Tanaka N, Calculating total acoustic power output using modal radiation efficiencies. *Journal of the Acoustical Society of America*. 1995; **97**: 1702-1709.
- [15] Van Mele, T., Panozzo, D., Sorkine-Hornung, O. and Block, P., Best-fit Thrust Network Analysis: Rationalization of freeform meshes. In S. Adriaenssens, P. Block, D. Veenendaal & C. Williams, (eds), *Shells for Architecture: Form finding and structural optimization*, Routledge Architecture, 2014.